

A Dual Input Converter to Hybridize Energy Sources Used in EV Applications

Resmi Ravindranath

PG Student dept. of Electrical and Electronics Engineering
Rajagiri School of Engineering and Technology Kerala, India

Renu George

Assistant Professor Dept. of Electrical and Electronics Engineering
Rajagiri School of Engineering and Technology Kerala, India

Caroline Ann Sam

Assistant Professor Dept. of Electrical and Electronics Engineering
Rajagiri School of Engineering and Technology Kerala, India

ABSTRACT

Anon-isolated dual input dc-dc converter that is useful for EV application is discussed in this paper. The converter combines two energy storage devices (supercapacitor and lead acid battery) using four switches, an inductor and a capacitor. This converter topology has a similar operation as that of a conventional DC-DC converter. Compared to other MIC topologies, the proposed converter has less output current ripple because of its high voltage gain. In this work, different operational modes, steady-state output equation and boundary condition of the converter is studied. The speed characteristics of BLDC motor using the converter is also analyzed in MATLAB/Simulink.

Index Terms—Multiple Input Converter (MIC), Energy Storage Systems (ESS), Hybrid Energy System (HES), Electric Vehicle (EV), power electronics

Date of Submission: 18-11-2022

Date of Acceptance: 02-12-2022

I. INTRODUCTION

Transportation sector has undergone major transformations over the years and one of the notable developments would be the shift from the conventional vehicles with IC engine to Electric Vehicles (EVs) and Hybrid Electric Vehicle (HEVs). With almost zero emission, EVs are efficient, and environment friendly transportation source.

Energy Storage Systems (ESS) is an integral part of every EV/HEV. They are devices that store, deliver or accept energy. Batteries and Supercapacitor are two most common ESS [2]. Batteries are electrochemical devices that convert electrical to chemical energy during charging and convert chemical to electrical energy during discharging. A battery cell consists of two electrodes immersed in an electrolyte. Even though the specific energy of battery is high, its specific power is relatively low. Hence, when battery alone is used as the ESS of an EV, it may fail to supply or absorb power with varying power requirement.

Supercapacitor or ultracapacitor are devices

with high specific power and lower specific energy compared to batteries. The lower specific energy, voltage dependence on the State of Charge (SOC) might possess problem when ultracapacitor is used alone as ESS. One of the best alternative is to integrate the two sources forming a Hybrid Energy System.

Hybrid Energy System (HES) is a technology that hybridizes more than two energy sources so as to compensate for the limitations of either of the sources and optimize the output. A power electronic circuit is necessary for the effective integration of the sources. Conventional methods use many independent Single-Input Converters connected to a common DC link as the interfacing circuit. It might lead to high-cost complex system with reduced efficiency and compactness. This led to the development of Multiple Input Converter (MIC).

MIC topologies developed in recent years help combine different energy sources with lesser number of components and produce regulated output. These MICs can deliver power all their input

sources either individually or simultaneously and have applications in many areas including EVs. Different PWM converter can either be connected in series or parallel to implement MIC. When connected in series, they produce regulated output voltage and continue to operate even if one of the input sources fails. When PWM converters are connected in parallel with or without electrical isolation, their control scheme would depend on the time-sharing concept due to clamped voltage. Hence, only one input source transfers power to the load at a time and, the simultaneous operation is not possible[3]. MICs are of isolated or non-isolated types. A MIC based on flux additivity integrates input sources in magnetic form instead of electric form. This converter uses PWM control to derive power from two input sources and deliver it to the load[4]. A Multiple-Input Isolated Bidirectional Dual Active Bridge DC-DC converter or MIIBDC is described in[5]. This configuration helps reduce circulation power and peak current stress in independent modes of operation. Even though isolated MIC provide electrical separation, the multi-winding transformer present makes these topologies costlier and complex compared to non-isolated types. A high gain MIC proposed in [6] consist of conventional buck-boost and boost converters. The stages preceding the last of the are buck-boost, while the last stage is a boost converter. This converter has switches with less current stress, and provides a wide control range for different input powers.

A three input DC-DC converter mentioned in [7] merges a fuel cell, a battery, and a PV for grid-connected applications. In this MIC, the fuel cell acts as the main power supply while the rooftop PV charges the battery, reduces fuel economy, and increases efficiency. Integration of energy sources play a pivotal role in sustainable development of vehicle electrification. Another MIC topology in[8] combines a battery and a supercapacitor for vehicular applications. This MIC can operate in buck, boost or buck-boost mode and, it is capable of drawing power from multiple energy sources to supply the vehicle load demand. A novel dual-input -single-out DC-DC converter is

considered in [9] and [10]. Even though the converter in [10] has a bridge arrangement, it will always have the presence of circulating current in input sources when any one of the switches is turned ON. The MIC presented in [11] has a fuzzy controller to integrate renewable energy sources to meet the load demand and produce a well-regulated output. Here a PWM inverter is used to provide the required energy to load. A multiple-input-multiple-output DC-DC converter is addressed in [12]. This topology produces multiple outputs with different voltage levels making it suitable for interfacing with multi-level inverters. The use of this inverter will reduce the harmonics which in turn reduces the torque ripple in the motor of an EV.

The topology studied in this paper is a non-isolated dual-input DC-DC converter connected in bridge configuration. This MIC hybridizes two energy sources effectively. The energy sources in the converter are connected in series using four semiconductor switches enabling bidirectional flow of power. The converter is designed for application in EV[1].

II. BRIDGE TYPE DUAL INPUT CONVERTER (BDC)

The converter accommodates two input energy sources namely a Supercapacitor (V_{S1}) and a Lead Acid Battery (V_{S2}) using an inductor, a capacitor and four IGBT switches (two with anti-parallel diodes and two without anti-parallel diodes). The principle of operation of the converter is same as that of a conventional DC-DC converter where the elements such as the inductor and the capacitor present store energy for a certain period and deliver it to the load for the rest of the period. The converter enables the energy sources to supply the power required by the load either individually or simultaneously with proper switching. Bidirectional power flow is possible in the converter. The proposed BDC has six modes of operation wherein the initial four modes consider power flow from source to load and the last two modes consider reverse power flow. The circuit diagram of the converter is represented in fig 1.

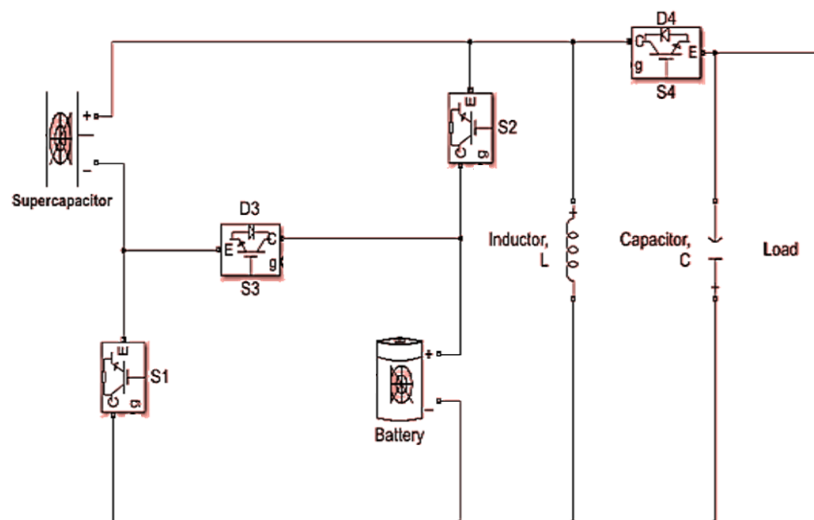


Fig 1: Proposed BDC

III. MODES OF OPERATION

The converter has six modes of operation. The first four modes consider power flow from the input sources to load. Modes 5 and 6 are generally for regenerative braking where power flows from load to source.

MODE1:In mode1, switch S1 conducts while other switches are OFF as in Fig. 2(a). Hence, inductor receives energy from the first source

V_{S1} (Supercapacitor).

MODE 2:In this mode, switch S3 is turned on which activates both the input sources as in Fig. 2(b). This allows both the sources to charge the inductor simultaneously. Because of this, the converter is suitable for EV application. During this mode of operation, switches S1, S2 and diode D4 are in OFF state.

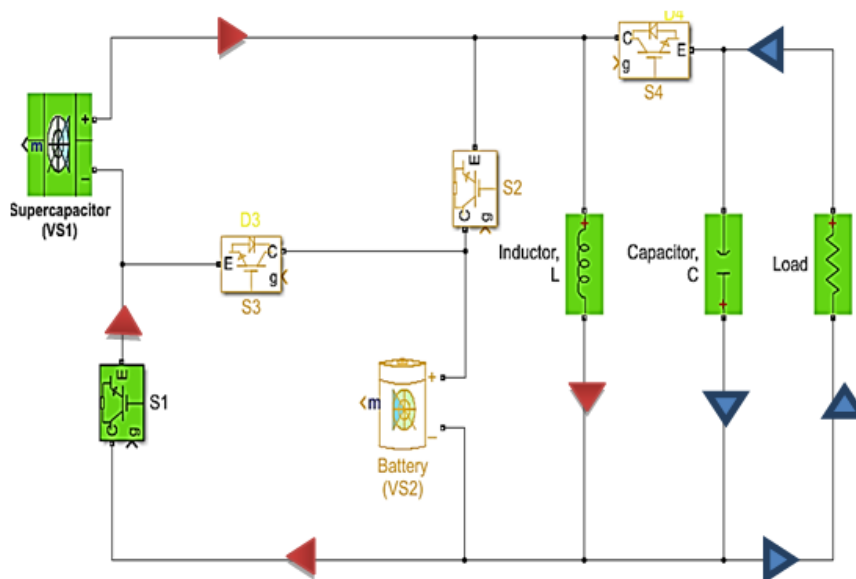


Fig. 2(a) Mode 1 operation of BDC

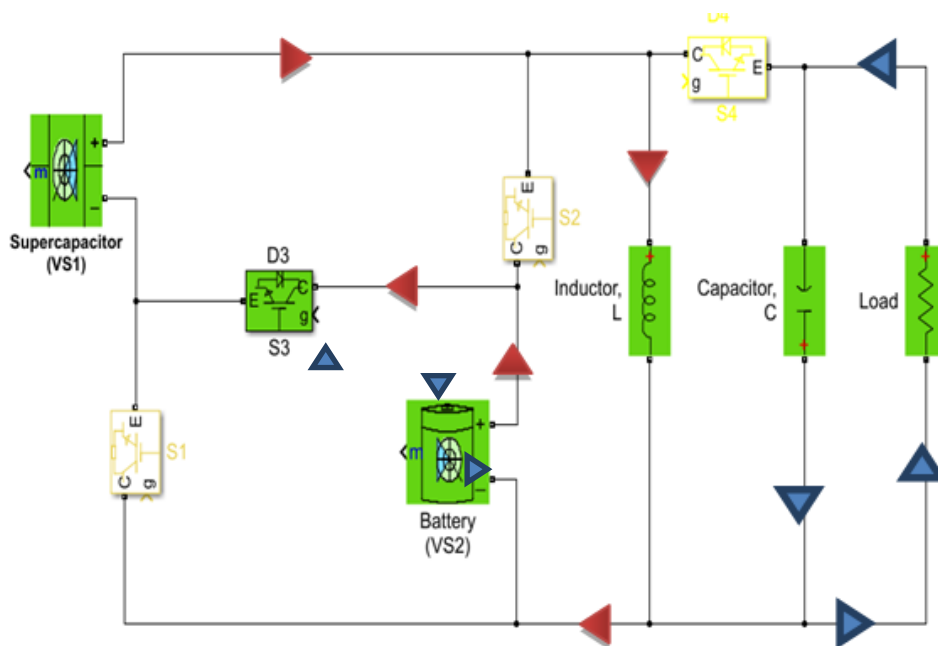


Fig. 2(b) Mode 2 operation of BDC

MODE 3: This mode consists of turning ON of switch S2 while keeping all other switches in OFF state as in Fig. 2(c). This activates the second source V_{S2} alone which in turn charges the inductor.

MODE 4: Here, all the switches are turned OFF as in Fig. 2(d). This causes the inductor to reverse its polarity and the energy stored in it is transferred to the load.

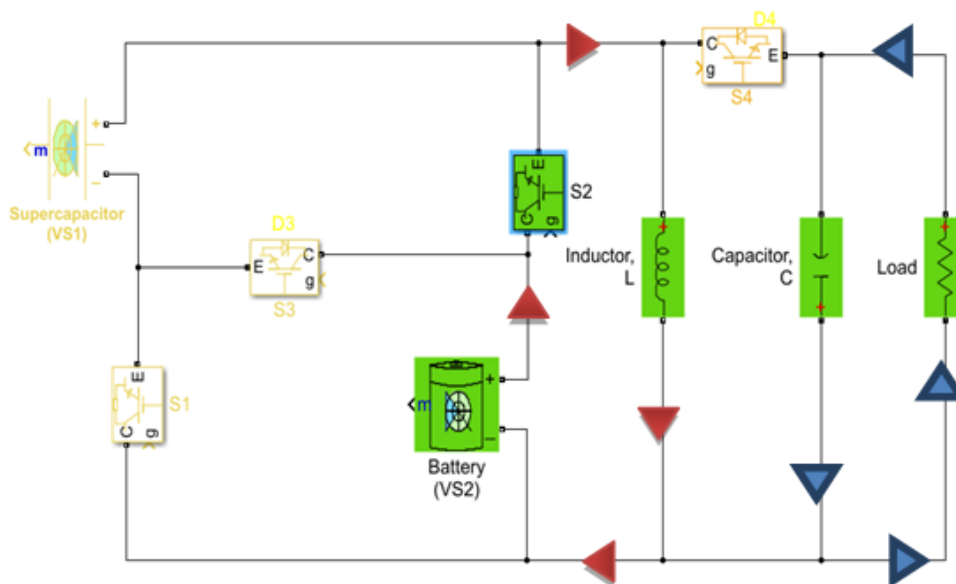


Fig. 2(c) Mode 3 operation of BDC

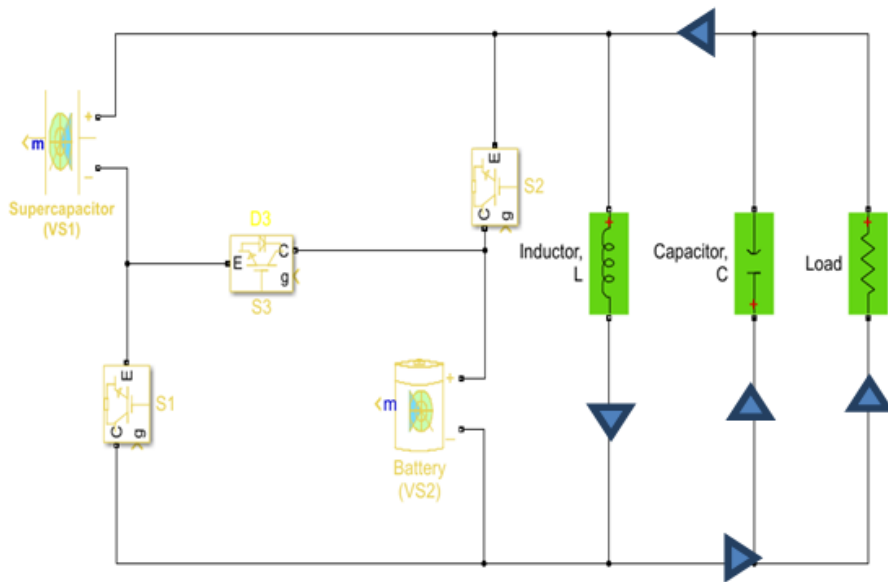


Fig. 2(d) Mode 4 operation of BDC

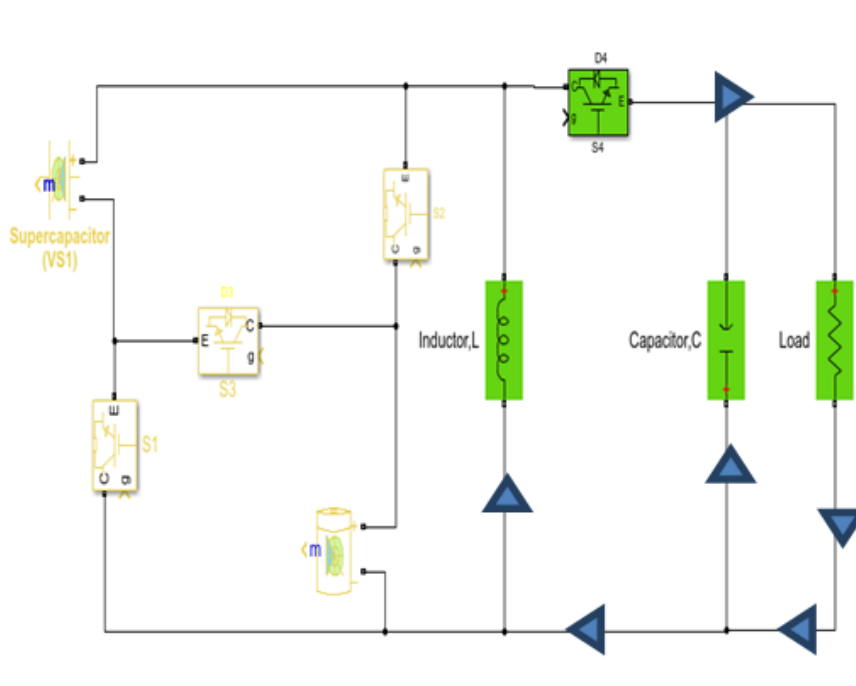


Fig. 2(e) Mode 5 operation of BDC

MODE 5: In this mode of operation switch S4 is turned ON as in Fig. 2(e). Thus, the inductor is charged to a level V_C by the load.

MODE 6: In the last mode of operation, switch S4 is turned OFF as in Fig. 2(f). The inductor reverses polarity and charges the input sources through diode D3. In mode 5 and mode 6 operation, switches S1, S2, and S3 are in OFF state.

Table I provides information on the operating modes of the converter.

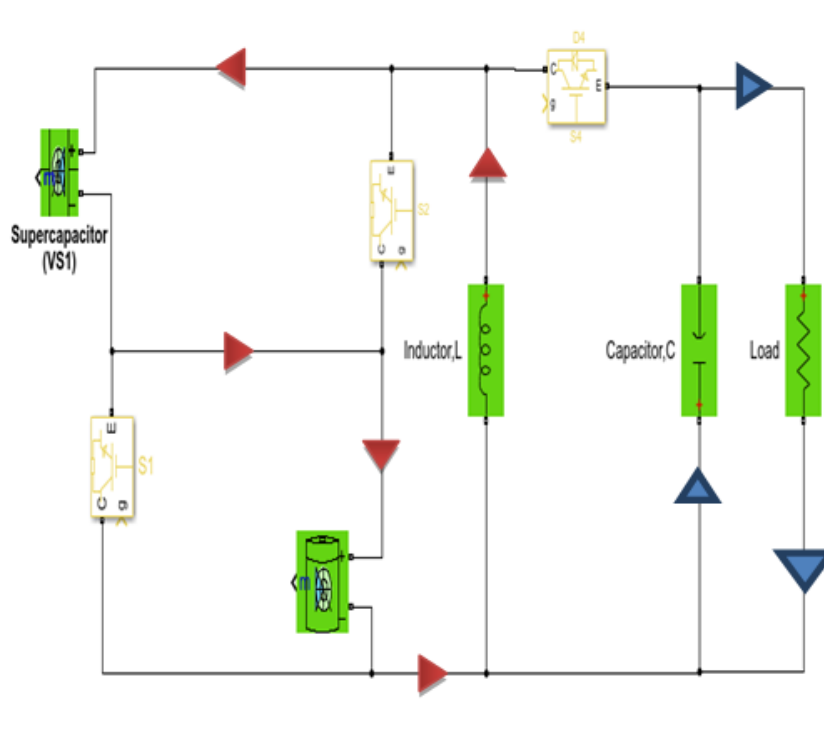


Fig. 2(f) Mode 6 operation of BDC

.TABLE 1
 MODES OF OPERATION OF BDC

MODE	SOURCE	SWITCH CONDUCTING	INDUCTOR VOLTAGE	STATUS OF INDUCTOR
Mode1	V_{S1}	S1	V_{S1}	Charging
Mode2	$V_{S1}+V_{S2}$	S3	$V_{S1}+V_{S2}$	Charging
Mode3	V_{S2}	S2	V_{S2}	Charging
Mode4	None of the sources are active	D4	$-V_C$	Discharging
Mode5	Load	S4	V_C	Charging
Mode6	$V_{S1}+V_{S2}$	D3	$V_{S1}+V_{S2}$	Discharging

IV. OUTPUT VOLTAGE EQUATION

The equation for output voltage of the BDC can be obtained from its steady state waveforms in [1].

Under steady-state operation, the average inductor current is taken to be zero. The average inductor voltage for a cycle is given by:

$$\int_0^{T_s} V_L \cdot dt = 0 \quad (1)$$

$$V_{S1}t_1 + V_{S2}t_2 + (V_{S1} + V_{S2})t_3 - V_C t_4 = 0 \quad (2)$$

$$t_1+t_2+t_3+t_4=T_s$$

$$\text{Hence, } t_4=T_s - (t_1+t_2+t_3) \quad (3)$$

$$\text{If } t_1=d_1T_s, t_2=d_2T_s \text{ and } t_3=d_3T_s$$

$$\text{Then } t_4=(1-(d_1+d_2+d_3))T_s$$

Substituting for $t_1, t_2, t_3,$ and t_4 in (2)

$$V_{S1}d_1T_s+V_{S2}d_2T_s+(V_{S1}+V_{S2})d_3T_s-V_C(1-(d_1+d_2+d_3))T_s=0 \quad (4)$$

Dividing (4) by T_s and replacing V_C with $-V_O$

$$V_{S1}d_1+V_{S2}d_2+(V_{S1}+V_{S2})d_3+V_O(1-(d_1+d_2+d_3))=0$$

$$-V_O(1-(d_1+d_2+d_3))=V_{S1}d_1+V_{S2}d_2+(V_{S1}+V_{S2})d_3$$

The output equation of the BDC when power from source to load is given by:

$$V_O = -\frac{V_{S1}d_1+V_{S2}d_2+(V_{S1}+V_{S2})d_3}{1-(d_1+d_2+d_3)} \quad (5)$$

The output voltage produced by the converter is negative. Hence, it is similar to a buck-boost converter. The negative voltage produced is a limitation of the BDC in comparison to other MICs.

The output voltage of the converter when power flows in the reverse manner [1] can be found by substituting the average inductor voltage to zero. i.e.

$$\int_0^{T_s} V_L \cdot dt = 0 \quad (6)$$

$$\text{In this case, the average inductor voltage over one cycle is : } V_C t_1 - (V_{S1}+V_{S2}) t_2 = 0 \quad (7)$$

$$\text{If } t_1 = DT_s \text{ and } t_2 = (1-d)T_s;$$

Then (7) can be written as:

$$V_C d T_s - ((V_{S1}+V_{S2})(1-d))T_s = 0 \quad (8)$$

Dividing (8) by T_s and replacing V_C with $-V_O$

$$-V_O d - ((V_{S1}+V_{S2})(1-d)) = 0$$

Therefore, output voltage when power flows from load source is:

$$V_{S1}+V_{S2}=\frac{-V_O d}{(1-d)} \quad (9)$$

During DCM operation, the inductor current starts from zero in mode 1 and approaches a maximum value of I_{LP2} by mode 3. In mode 4, all switches are in OFF state and inductor reverses its polarity. This makes the inductor to deliver the energy stored in it to the load side for a period $d_x T_s$. The inductor current reduces to zero by the end of this mode as the energy stored in it is completely discharged. In mode 5, the load is supplied by the energy stored in the capacitor.

The boundary condition between CCM and DCM is found by substituting $V_{S2} = yV_{S2} = yV_{in}$, where y is known as the scaling factor.

Substituting for V_{S1} and V_{S2} and replacing V_O with $-V_C$ in (5)

$$V_C = \frac{(V_{in})d_1 + y(V_{in})d_2 + (V_{in} + yV_{in})d_3}{1 - (d_1 + d_2 + d_3)}$$

$$V_C = V_{in} \frac{d_1 + yd_2 + (1 + y)d_3}{1 - (d_1 + d_2 + d_3)}$$

The voltage-gain of the converter during CCM and DCM operations are:

$$G_{CCM} = \frac{V_C}{V_{in}} = \frac{d_1 + yd_2 + (1 + y)d_3}{1 - (d_1 + d_2 + d_3)} \quad (10)$$

$$G_{DCM} = \frac{V_C}{V_{in}} = \frac{d_1 + yd_2 + (1 + y)d_3}{\sqrt{2\tau_L}} \quad (11)$$

Where τ_L is known as the normalized time constant and is equal to $\frac{Lf_s}{R}$. Here R is the load resistance.

To find the boundary condition [1], substitute $G_{CCM} = G_{DCM}$, then,

$$\frac{d_1 + yd_2 + (1 + y)d_3}{1 - (d_1 + d_2 + d_3)} = \frac{d_1 + yd_2 + (1 + y)d_3}{\sqrt{2\tau_{LB}}}$$

$$1 - (d_1 + d_2 + d_3) = \sqrt{2\tau_{LB}}$$

Squaring both sides

$$(1 - D)^2 = 2\tau_{LB}$$

Hence, the boundary normalized time constant is expressed as:

$$\tau_{LB} = \frac{(1 - D)^2}{2} \quad (12)$$

where $D = d_1 + d_2 + d_3$

The variation of τ_{LB} for differing values of D is shown in Fig.3.

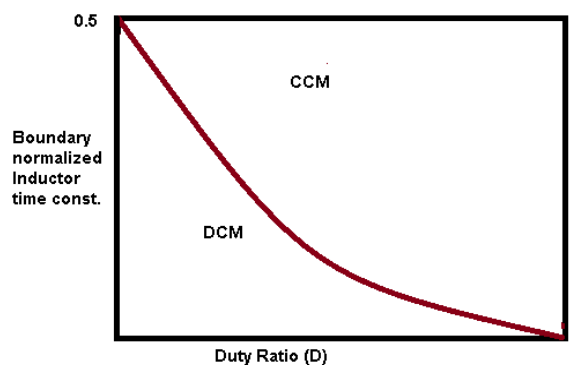


Fig 3: Boundary condition of BDC

V. DESIGN

A. Design of Inductor

Assuming the power absorbed by the load is the same as that supplied by source.

$$\text{Output power, } P_O = \frac{V_O^2}{R} \quad (13)$$

$$\text{Power supplied by source, } P_S = V_S I_S \quad (14)$$

$$\text{Where } V_S = V_{S1} + V_{S2}$$

(13) is equal to (14)

$$\frac{V_O^2}{R} = V_S I_S \quad (15)$$

Average source current (I_S) and average Inductor current (I_L) are related by the equation

$$I_S = I_L D \quad (16)$$

Substituting (16) in (15)

$$\frac{V_O^2}{R} = V_S I_L D$$

$$\text{Hence, } I_L = \frac{V_O^2}{R D V_S} \quad (17)$$

Assuming duty ratios d_1 and d_2 are equal and substituting for V_O from (5)

$$I_L = \frac{V_S (D+d_3)^2}{4RD (1-D)^2} \quad (18)$$

$$\text{Maximum Inductor current, } I_{\max} = I_L + \frac{\Delta i_L}{2}$$

$$\text{Hence, } I_{\max} = \frac{V_S (D+d_3)^2}{4RD (1-D)^2} + \frac{D V_S}{2L f_S}$$

$$\text{Minimum Inductor current, } I_{\min} = I_L - \frac{\Delta i_L}{2}$$

$$I_{\min} = \frac{V_S (D+d_3)^2}{4RD (1-D)^2} - \frac{D V_S}{2L f_S}$$

To ensure continuous current, Inductor current must be positive.

Setting I_{\min} to zero,

$$I_L = \frac{\Delta i_L}{2}$$

$$\text{That is: } \frac{V_S (D+d_3)^2}{4RD (1-D)^2} = \frac{D V_S}{2L_{\min} f_S}$$

Hence, the minimum Inductance,

$$L_{\min} = \frac{2RD^2(1-D)^2}{f_s(D+d_3)^2} \quad (19)$$

The value of Inductance for the converter should be greater than L_{\min}

B. Design of Capacitor

Change in charge,

$$\Delta Q = I_o DT_s = \frac{DT_s V_o}{R} = C \Delta V_o$$

Therefore,

$$\Delta V_o = \frac{DT_s V_o}{RC} = \frac{DV_o}{RC f_s}$$

Therefore, the minimum capacitance,

$$C = \frac{D}{R(\Delta V_o/V_o)f_s} \quad (20)$$

Where $\frac{\Delta V_o}{V_o}$ is the voltage ripple. The value of capacitance for the converter should be greater than the minimum capacitance.

VI. SIMULATIONS AND RESULTS

The simulations for the open-loop and the closed-loop control of the proposed converter are performed using MATLAB/Simulink.

Unidirectional power flow (from the source to the load) is considered in this paper. The specifications for parameters used in open-loop control and closed-loop control is given in Table II and III.

TABLE II
 PARAMETERS FOR SIMULATION OF OPEN-LOOP CONTROL

PARAMETERS	SPECIFICATION
Source1 (Supercapacitor)	48V rated
Source2 (Battery)	36V,5A
Inductor (L)	2mH
Capacitor (C)	22 μ F
Switching frequency	20kHz
Load Resistor	160 Ω

For open-loop control, the simulations are carried out by taking the duty ratios d_1 as 20%, d_2 as 20% and d_3 as 23.5% to get an output of 100V. Fig. 4(a) shows the simulation diagram of BDC under open-

loop control. The inductor voltage and output voltage waveforms of open-loop control are shown in fig. 4(b) and 4(c).

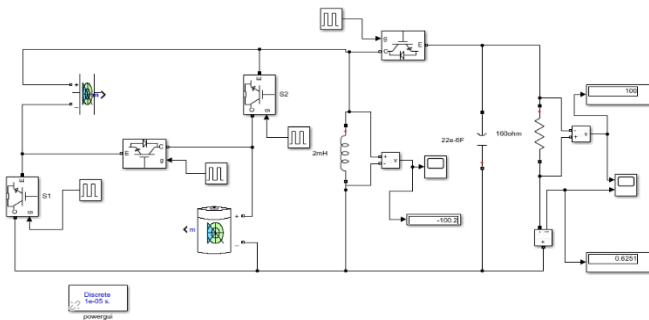


Fig 4 (a): Simulation dig. of the proposed converter

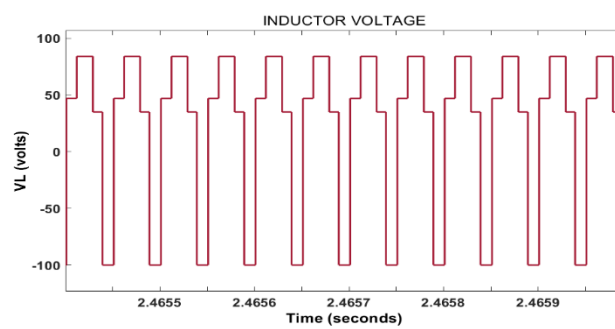


Fig 4 (b): Simulation result for open-loop control: Inductor Voltage

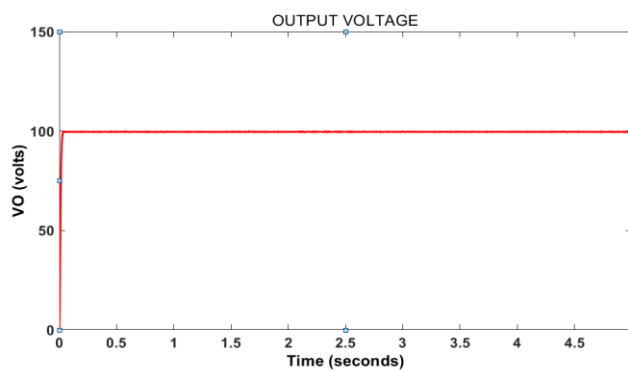


Fig 4 (c): Simulation result for open-loop control: Output Voltage

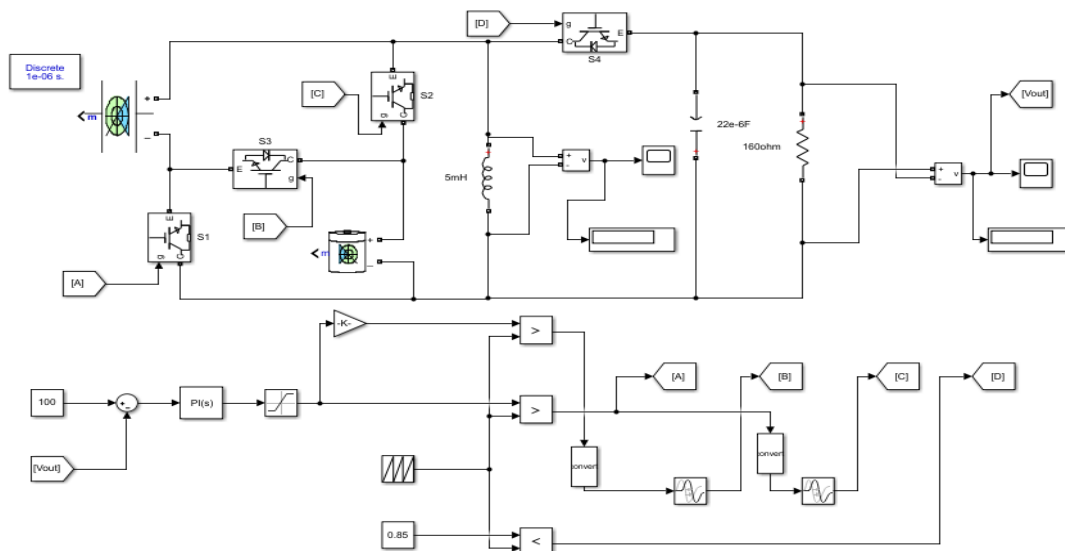


Fig 4 (d): Simulation dig. for closed-loop control of BDC

TABLE III
 PRAMETERS FOR CLOSED-LOOP CONTROL

PARAMETERS	SPECIFICATION
Source1	48V (rated)
Source2	36V, 5A
Inductor (L)	5mH
Capacitor (C)	22µF
Switching frequency	20kHz
Load Resistor	160Ω

Fig. 4(d) shows the simulation diagram for closed-loop control of BDC. The difference in the actual and reference voltage during closed-loop control is summarized in Table IV.

TABLE IV
 SIMULATION RESULTS FOR CLOSED-LOOP CONTROL

REFERENCEVOLTAGE (V)	ACTUAL VOLTAGE (V)
36	35.77
48	48.09
60	59.31
80	79.2
100	99.8

From Table IV, it can be seen that the actual and reference voltage during closed-loop control is either minimum or nil. Fig. 4(e) represents the inductor voltage waveform during close loop control for a reference voltage of 100V.

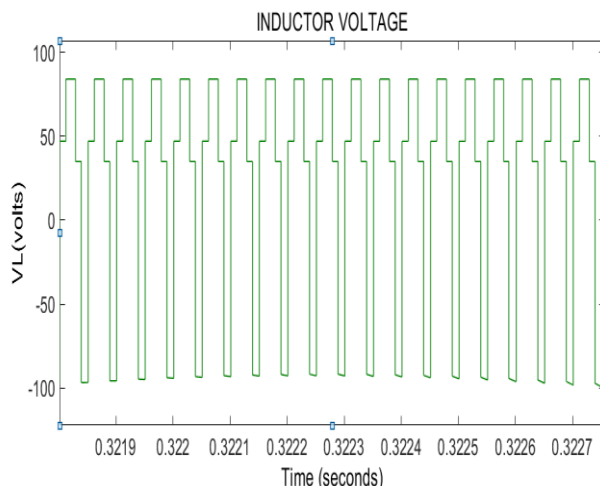


Fig 4(e): Inductor voltage waveform for reference voltage of 100V

The speed performance for different speeds of BLDC motor using the converter is also analyzed in MATLAB/Simulink platform. The parameters used for the same is summarized in Table V.

TABLE V
 PARAMETERS FOR SIMULATION

PARAMETERS	SPECIFICATION
Source1 (Supercapacitor)	48V (rated)
Source2 (Battery)	36V, 5A
Inductor (L)	5mH
Capacitor (C)	23 μ F
Switching frequency	20kHz
Inverter switches	MOSFET/Diode

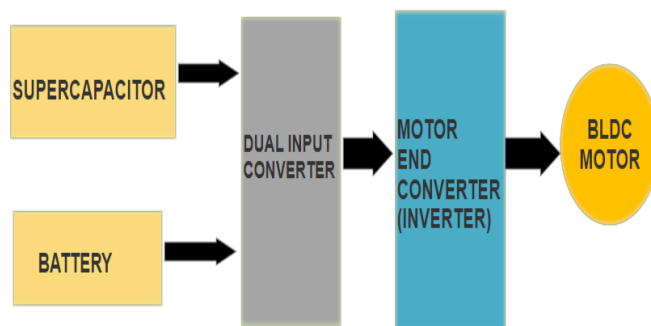


Fig 5(a): Block diagram of the converter

The simulations are done as in the block diagram given in Fig.5(a). The control of the converter is designed in a manner that the Battery source alone is active for lower speed ranges (up to 400rpm), for medium speed ranges (400rpm to 1000rpm), Super capacitor provides the required input to the converter, and, for higher speed ranges (up to 1500) both the sources are made to operate simultaneously. A universal bridge with MOSFET/Diodes is used as the inverter in the

simulation. The control of the inverter is done such that two switches conduct at a time. Fig 5(b) is the control of the proposed converter section. Fig. 5(c) shows the simulation diagram for speed control of BLDC motor. The results are given in Table VI.

The results in Table VI verifies that the converter is suitable for speed control of the BLDC motor. The speed-time waveforms obtained for 300rpm, and 1500 rpm are shown in Figures 5(d), and 5(e) respectively.

TABLE VI
 SIMULATION RESULTS

ACTIVE SWITCH	SOURCE	REF. SPEED (rpm)	ACTUAL SPEED (rpm)
S2	Battery	300	300
S1	Super capacitor	600	600
S1	Super capacitor	800	799.7
S1	Super capacitor	1000	999.8
S3	Both Sources	1500	1500

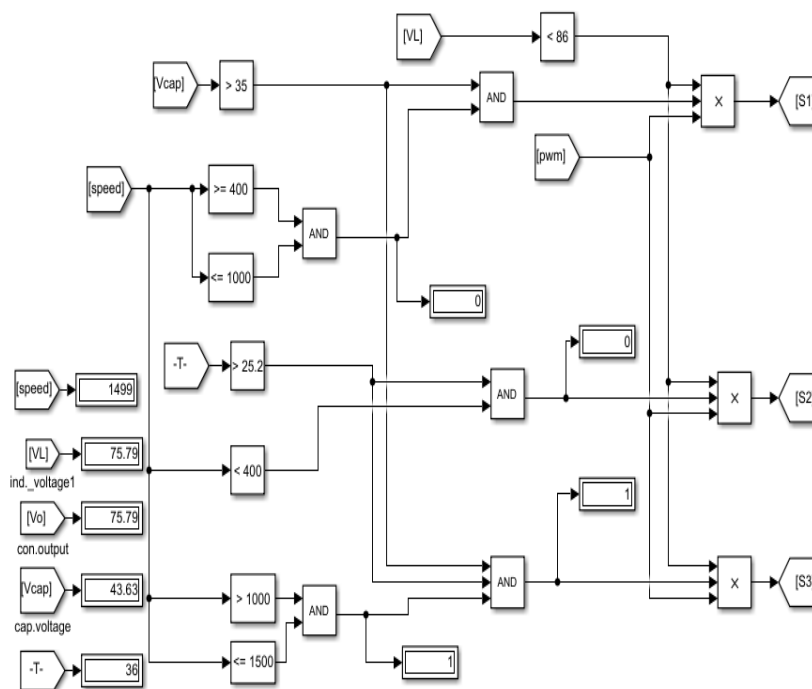


Fig. 5(b): Control section

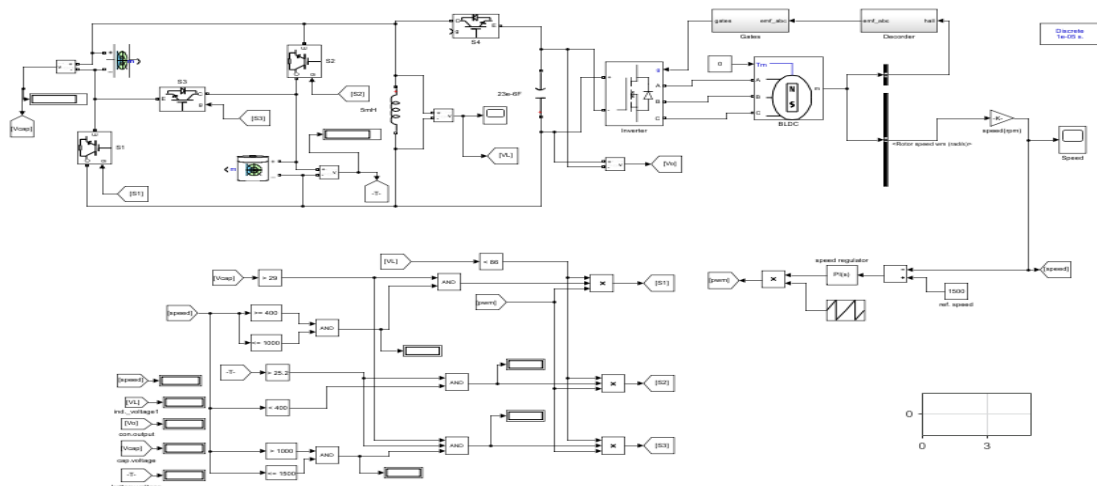


Fig. 5(c): Simulation dig. for speed control of BLDC motor using the converter

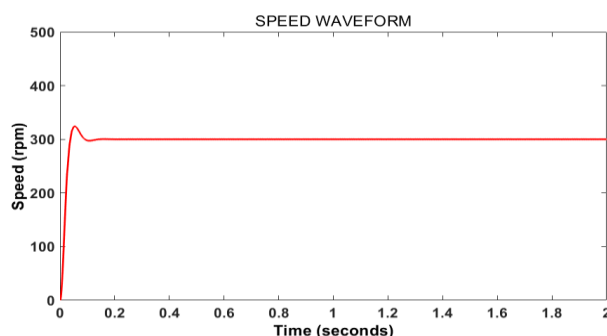


Fig. 5(d): Waveform for speed of 300rpm

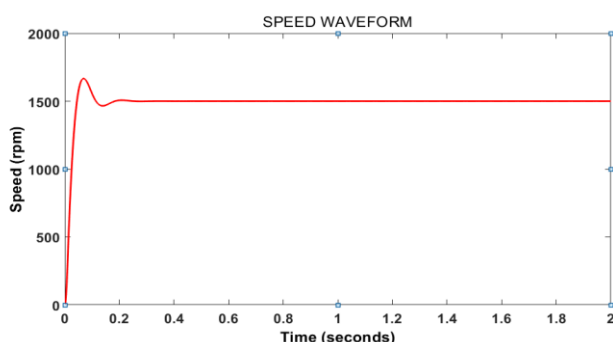


Fig 5(e): Waveform for speed of 1500rpm

VII. HARDWARE SETUP

A prototype of the proposed using input voltages of 6V and 12V has been developed in a laboratory environment. In the model, the switches are realized using four IRF840 MOSFETs and a ceramic cement resistor becomes the load. Four isolated TLP250H driver ICs are used to drive the

switches. Close loop control of the converter is made possible with dsPIC30F2010 controller. Fig. 6(a), 6(b), 6(c) and 6(d) shows the hardware setup of the BDC, its input waveforms and output waveform respectively. The result of close loop control is summarized in Table VII.

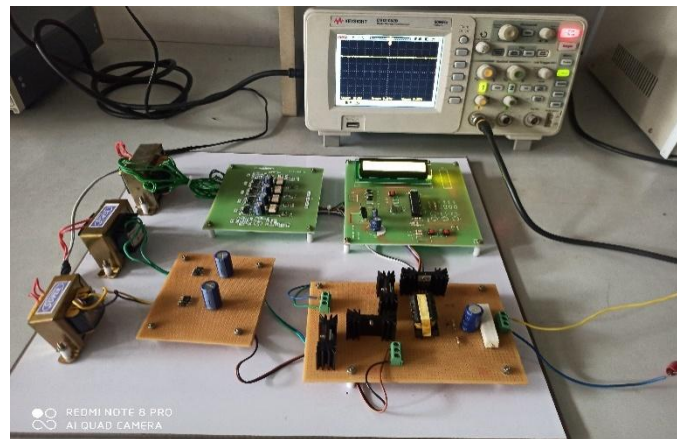


Fig. 6(a): Hardware Setup

TABLE VII
HARDWARE RESULTS

REFERENCE VOLTAGE (V)	ACTUAL VOLTAGE (V)
7.6	7.7
11.2	11.4
13.5	13.5
14.7	14.7
15.9	16
20	20.2
24.2	24.3

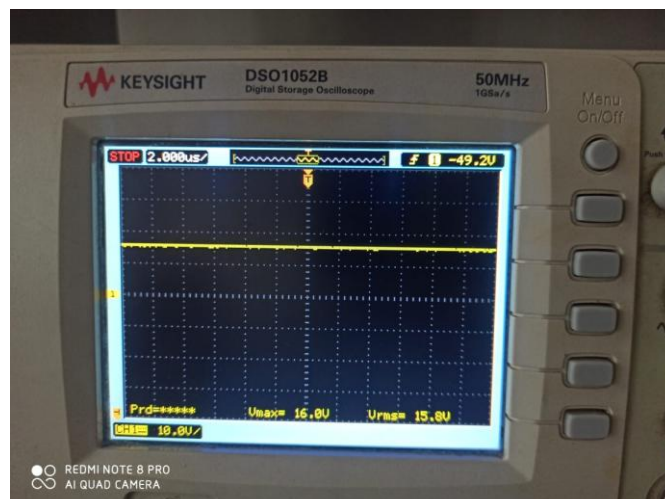


Fig. 6(b): V_{S1} Waveform

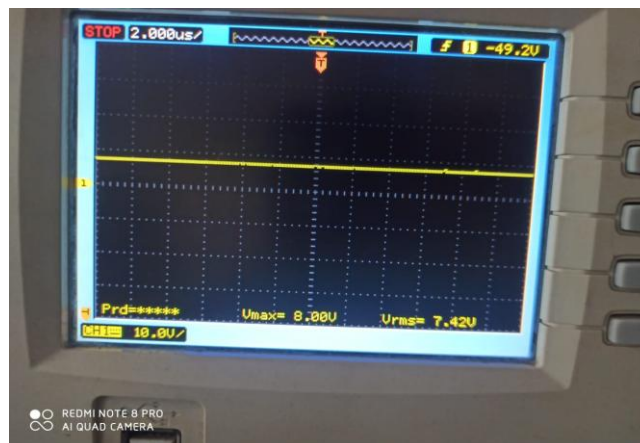


Fig. 6(c): V_{S2} Waveform



Fig. 6(d): Output waveform for an actual voltage of 11.4V

VIII. CONCLUSION

A dual input converter to integrate a Supercapacitor and a Battery source is discussed in this paper. The proposed converter allows bidirectional power flow. It also allows individual or simultaneous energy utilization from the input sources. The converter has an output equation similar to that of a conventional buck-boost converter, hence, it is capable of stepping down or boosting the output depending on the requirements. The simulation results also verify the same. The converter can be used to effectively control the speed of BLDC motor. Integration of input sources with lesser number of components, and simultaneous operation of both sources are the potential advantages making for EV applications.

REFERENCE

- [1]. A.Sivaprasad, G.G. Kumar, S. Kumaravel, S. Ashok, "A Non-Isolated Bridge-Type DC-DC Converter for Hybrid Energy Source Integration," *IEEE Trans. Industry Appl.*, vol. 55, no. 4, July/August 2019.
- [2]. A. Ostadi, S.K. Chen, "Hybrid Energy Storage System (HESS) in Vehicular Applications: A Review on Interfacing Battery and Ultra-capacitor Units," *ITEC June 2013*, doi: 10.1109/ITEC.2013.6573471.
- [3]. Y. C. Liu and Y. M. Chen, "A systematic approach to synthesizing multi-input DC/DC converters," in *Proc. Power Electron. Spec. Conf.*, Orlando, FL, USA, 2007, pp. 2626–2632.
- [4]. Y.M. Chen, Y.C. Liu, and F.Y. Wu, "Multi-input DC/DC converter based on the multi winding transformer for renewable energy applications," *IEEE Trans. Ind. Appl.*, vol. 38, no. 4, pp. 1096–1104, Jul./Aug. 2012.
- [5]. V. Karthikeyan and R. Gupta, "Multiple-input configuration of isolated bidirectional DC-DC converter for power flow control in combinational battery storage," *IEEE Trans. Ind. Informat.*, vol. 14, no. 1, pp. 2–11, Jan. 2018.
- [6]. M. R. Banaei, H. Ardi, R. Alizadeh, and A. Farakhor, "Non-isolated multi-input-single-output DC/DC converter for photovoltaic power generation systems," *IET Power Electron.*, vol. 7, no. 11, pp. 2806–2816, Nov. 2014.

- [7]. R. R. Ahrabi, H. Ardi, M. Elmi, and A. Ajami, "A novel step-up multi-input DC–DC converter for hybrid electric vehicles application," *IEEE Trans. Power Electron.*, vol. 32, no. 5, pp. 3549–3561, May 2017.
- [8]. L. Kumar and S. Jain, "A novel dual input DC/DC converter topology," in *Proc. IEEE Int. Conf. Power Electron. Drives Energy Syst.*, Bengaluru, India, pp. 1–6, 2012.
- [9]. L. Kumar and S. Jain, "A novel dual input DC/DC converter topology," in *Proc. IEEE Int. Conf. Power Electron. Drives Energy Syst.*, Bengaluru, India, pp. 1–6, 2012.
- [10]. A. Sivaprasad, G. G. Kumar, S. Kumaravel, and S. Ashok, "Performance analysis of novel bridge type dual input DC-DC converters," *IEEE Access*, vol. 5, pp. 15340–15353, Aug. 2017.
- [11]. P. R. Shiyas, S. Kumaravel, and S. Ashok, "Fuzzy controlled dual input DC/DC converter for solar- PV/Wind hybrid energy system," in *Proc. Students IEEE Conf. Elect. Electron. Comput. Sci.*, Bhopal, India, pp. 1–5, 2012.
- [12]. A. Nahavandi, M. T. Hagh, M. B. B. Sharifian, and S. Danyali, "A non-isolated multi-input multi-output DC–DC boost converter for electric vehicle applications," *IEEE Trans. Power Electron.*, vol. 30, no. 4, pp. 1818–1835, Apr. 2015.